ELSEVIER

Biochimica et Biophysica Acta 1420 (1999) 139–152

BIOCHIMICA ET BIOPHYSICA ACTA
BBA

www.elsevier.com/locate/bba

Pore-forming action of mastoparan peptides on liposomes: a quantitative analysis

Anna Arbuzova [1], Gerhard Schwarz *

Department of Biophysical Chemistry, Biocenter of the University of Basle, Klingelbergstrasse 70, CH-4056 Basle, Switzerland

Received 17 February 1999; received in revised form 12 May 1999; accepted 2 June 1999

Abstract

We have investigated the wasp venom peptides mastoparan X and polistes mastoparan regarding their apparent potential to induce pore-like defects in phosphatidylcholine unilamellar vesicles. Based on a fundamental theoretical model, the pore activation and deactivation kinetics have been evaluated from the observed efflux of liposome entrapped carboxyfluorescein in relation to the bound peptide to lipid ratio. We can quantitatively describe our experimental data very well in terms of a specific reaction scheme resulting in only a few short-lived pores. They evidently emerge rapidly from a prepore nucleus being produced by two rate-limiting monomeric states of bound peptide. These peculiar states would be favorably populated in an early stage of bilayer perturbation, but tend to die out in the course of a peptide/lipid restabilization process.

Keywords: Lipid vesicle; Mastoparan peptide; Binding curve; Mode of efflux; Pore formation; Kinetic mechanism

1. Introduction

The mastoparans, being toxic tetradecapeptides from the venom of various wasp species, are known to exert manifold biologically significant molecular functions. They cause degranulation of mast cells [1–3], mimic part of a G-protein receptor [4] and stimulate the activity of phospholipase A_2 [5]. More recently, it has been shown that mastoparan inhibits Golgi vesicle transport in vitro by directly perturbing the membrane [6]. By all means, these peptides generally cause a substantial lipid bilayer permeability for hydrophilic material [5,7–9]. The same phenomenon has actually been observed with a multitude of other amphiphilic agents, particularly peptides. It can experimentally be studied by measuring the induced efflux kinetics of an appropriate marker substance out of liposomes. The fact that usually even a rather small amount of such an agent results in a noticeable leakage has led to the concept of induced 'pores', i.e. isolated defects of the membrane structure where polar molecules can pass through quite freely. Such pore activity has generally been found to undergo a dramatic slowing down within minutes. This very peculiar point apparently suggests that the conditions for open pores are especially favorable immediately after having added the pore-forming agent, but fall off substantially afterwards. It calls for a reasonable explanation in any attempt of a quantitative analysis.

* Corresponding author. Fax: +41-61-267-2189; E-mail: schwarzg@ubaclu.unibas.ch.

[1] Present address: Department of Physiology and Biophysics, State University of New York, Stony Brook, NY 11794-8661, USA.

0005-2736/99/$ – see front matter
PII: S0005-2736(99)00098-X

In many respects, the mastoparans resemble the somewhat larger peptide melittin of bee venom [10]. They also adopt a largely α-helical conformation when having associated with the lipid bilayer [11,12]. All these peptides have an amphipathic nature which implies a segregation of polar and apolar faces of the helix. Such a feature has given rise to the idea that cell membrane channels are made up by bundles of peptide sequences forming transmembrane amphipathic helices that surround a central pore, the so-called 'barrel-stave' model [13–15]. Pores induced by melittin have also been discussed on this basis. However, in contrast to melittin (being composed of 26 amino acid residues), mastoparans in their α-helical state are definitely not long enough to span a lipid bilayer. Nevertheless, mastoparan induced pores have been clearly identified in planar lipid membranes by means of electrical conductance experiments [16]. Their actual architecture remains so far obscure. Anyway, the bulk of bound mastoparan molecules should lie on the membrane surface with their polar (charged) face oriented towards the aqueous medium [11,12] in the same way as maintained for melittin [17]. By no means, however, would this rule out that some of the peptide penetrates deeper into the core of the bilayer when forming pores, since only a small fraction of the lipid-associated peptide should be needed in such an action.

The self-quenching fluorescent dye carboxyfluorescein (CF) has become very popular as a marker for efflux experiments [18,19]. In order to utilize the measured signal towards a quantitative analysis of the underlying molecular mechanism of pore formation it will be necessary to convert the observed time course of fluorescence dequenching upon marker release into a reasonably defined pore opening rate. This quantity should then be discussed as a function of the actual bound peptide-to-lipid ratio.

In our laboratory, we have developed a theoretical basis to convert the empirical efflux signal in a pertinent way. A comprehensive report describing it in greater detail with regard to melittin has been given elsewhere [20]. The present article follows essentially the same route for two mastoparan species, namely: mastoparan X (MPX), $^{+}$INW^{+}KGIAAMA^{+}K^{+}-KLL-NH_2; and polistes mastoparan (MPP), $^{+}$V^{-}DW^{+}K^{+}KIGQHILSVL-NH_2 carrying the indicated positive and negative charges at neutral pH. The apparent dynamics of the pore formation turns out to be rather concurrent with that of melittin, although there are some specific differences of interest. Anyway, a basic barrel-stave model of the mastoparan pore cannot easily be visualized in view of the fact that an α-helical conformation of this peptide fails to span the membrane.

2. Materials and methods

2.1. Substances

We used a standard HEPES buffer consisting of 100 mM NaCl, 10 mH HEPES, 1 mM EDTA and approximately 5.6 mH NaOH adjusted to pH 7.4 at 20°C. HEPES was from Bioprobe (Chemie Brunschwig, Basle, Switzerland). Triton X-100, NaCl, Tris and EDTA were supplied by Merck (Darmstadt, Germany). Proteinase K was a product of Boehringer Mannheim (Mannheim, Germany). The fluorescent agents 5(6)-carboxyfluorescein (CF) (mixed isomers, MW 376.3, 99% pure by HPLC) and FITC-dextran (MW 9400) were bought from Sigma (St. Louis, MO, USA). The lipids POPC, DOPC, DOPS being dissolved in chloroform were obtained from Avanti Polar Lipids (Birmingham, AL, USA). They have been used without further purification. Lipid concentration in stock solution was determined by phosphate analysis [21]. The labeled lipid NBD-DPPE was supplied by Molecular Probes (Europe BV, Leiden, Holland). Synthetic samples of mastoparan X and polistes mastoparan were obtained from Bachem Feinchemikalien (Bubendorf BL, Switzerland). Their concentrations in stock solution have been measured by means of the Trp optical absorption (5570 cm^{-1} M^{-1} at 280 nm). Individual portions taken from stock solution have been kept in Eppendorf caps at −20°C until they were used immediately in an experiment.

2.2. Liposomes

Small unilamellar lipid vesicles (SUV) were prepared in the conventional way by ultrasonic irradiation using a microtip sonicator (MSE ultrasonic disintegrator) with a cooling bath of 10°C. Our detailed procedure is the same as described elsewhere [22].

Gel filtration (by means of a Sepharose CL4B column) was applied to separate the major fraction of small vesicles. Large unilamellar lipid vesicles (LUV) were prepared by means of the extrusion technique [23,24] using a 100-nm polycarbonate membrane (Nucleopore, Pleasanton CA, USA) at 15-bar N_2 pressure. Some apparent fraction of multilamellar vesicles was separated by centrifugation. The stock solution was stored at 4°C.

Vesicle sizes have been determined using dynamic light scattering as described previously [20]. This revealed average radii of 12 ± 2 nm for the SUV and 50 ± 3 nm for the LUV. According to the geometric packing constraints of the individual molecules [25], the number of lipid molecules per vesicle thus amounts to about $N_L = 3500$ and $N_L = 87\,000$, respectively. Marker-entrapped vesicles were prepared with a standard stock solution (stored at −20°C) consisting of 50 mM CF, 10 mM HEPES, 10 mM NaCl, 1 mM EDTA and approximately 135 mM NaOH that has the same pH and osmolarity as the standard buffer. For measurements of the static quenching curves the dye stock solution was diluted to lower concentrations with the standard buffer. The concentration of dye was checked by optical absorption (72 000 M^{-1} cm^{-1} at 490 nm). External dye was removed by gel filtration through a Sephadex G-50 or G-75 column (1×30 cm) for LUV and a Sepharose CL4B (1×30 cm) for SUV.

Vesicles with 0.3–0.5 mol% NBD-PE were prepared in the same way after having mixed the proper amount of lipids in chloroform. NBD-PE inner layer labeled liposomes were produced by reducing NBD on the outer leaflet [26], applying approximately 10 mM Na-dithionite (from Fluka BioChemika, Buchs, Switzerland) for 5 mM lipid. Monitoring the fluorescence of the NBD group (excitation at 460 nm, emission at 536 nm) showed a 50% reduction of the initial fluorescence intensity within 5 min. All our fluorescence measurements in this work were done on a spectrofluorometer FP 777 (Jasco, Tokyo, Japan).

Liposomes generally exist in a metastable state that is difficult to be reproduced precisely. Apparently, there is a certain margin of structural defects in the lipid bilayer resulting in a somewhat extended variability of peptide binding and permeability. As already discussed previously [20], any reliable quantitative analysis thus requires a reasonable averaging procedure based on experiments with a greater number of reiterated vesicle preparations.

The SUV turned out to undergo a slow tendency of becoming unstable and to fuse or aggregate even without any peptide. Therefore, they were used only the same day they were prepared. On the other hand, extruded LUV proved to be stable and retained their size with and without peptide for weeks.

2.3. Peptide binding

The partitioning of aqueous peptide into the lipid bilayer phase was determined through the fluorescence increase of the peptide's tryptophan residue: excitation 280 nm (slit 1.5 nm); emission 320 nm (slit 3 nm) measured in 0.5 cm cuvettes at 20°C. A peptide solution was titrated with lipid vesicles. We employed a quite comprehensive data-processing routine that includes a large number of measurements with a series of different peptide concentrations taking into account corrections for dilution and light scattering. The method has been described elsewhere in great detail [27]. At low concentrations of peptide, there may be some loss of it due to sticking on the walls. This effect could be remedied for by presaturating the cuvette with the same concentration used afterwards in the actual experiments. Following our established theoretical approach [27–30], an association isotherm ('binding curve') can be derived as

$$r = (K_p/\alpha)\cdot c_f, \quad \ln \alpha = 2z\cdot\sinh^{-1}(zbr) \qquad (1)$$

expressing r, the ratio of bound peptide per lipid, as a function of c_f, the concentration of free peptide in the aqueous phase. The ideal partition coefficient, K_p, is a measure of the 'binding' affinity to the lipid bilayer, whereas the activity coefficient, α, takes into account the repulsive electrostatic interactions of the positively charged peptide molecules as they get rather close to each other in the membrane associated state. The parameter z stands for an effective charge number per monomer and b is a constant factor depending on the ionic strength of the buffer. Whether bound peptide would translocate across the liposomal membrane has been investigated using a method proposed by Maduke and Roise [31]. MPX was added to NBD-PE symmetrically labeled vesicles and the binding was monitored by means of the flu-

orescence energy transfer between tryptophan and NBD (excitation 280 nm, emission 536 nm). After some time, an amount of the order of 20–40 μg proteinase K was added to digest the peptide on the outer leaflet. The amount still bound on the inner leaflet (not digestible within 3–5 min) was then determined from the reduced plateau value of the fluorescence signal. Instead of digestion by protease, an excess of lipid (about five times higher than the initial lipid concentration) could be added to remove peptides bound to the outer leaflet. In this case, the results had to be corrected for lipid fluorescence and light scattering. These experiments were done with the LUV only.

Also for the LUV, a possible lipid flip-flop caused by bound peptide has been checked adopting a method proposed by other authors [26,32]. Briefly, MPX was incubated with asymmetrically labeled vesicles (NBD-PE only on the inner leaflet). Having waited some time, we first added 40 μg proteinase K (20 μl of 2 mg/ml stock solution) to digest the peptide and after 3–5 more minutes NBD on the outer leaflet was reduced by means of Na-dithionite. The part of NBD labeled lipid that has flipped within this time to the outer leaflet can so be determined from normalizing the NBD fluorescence (excitation 460 nm, emission 536 nm).

2.4. Marker efflux

The release of vesicle entrapped CF that is induced by the interaction with peptide has been monitored as a dequenching signal upon dilution into the extravesicular domain. Vesicles were dissolved in 2 ml standard buffer (at a final lipid concentration that ranged between about 15 and 200 μM) using a 1-cm quartz cuvette. Then the peptide was added (0.1–4 μM). We preferred this order of mixing both components since one can so easily measure the initial fluorescence of the fully entrapped dye. Tests with a reversed sequence of mixing revealed no significant differences of the efflux curves (provided the cuvette walls had been presaturated with peptide). Increase of the fluorescence intensity $F(t)$ (at 520 nm, slit 5 or 10 nm; excitation at 490 nm, slit 1.5 nm) was recorded as a function of time t while stirring the solution. A typical time course of $F(t)$ is shown in Fig. 1. We have always normalized it towards an experimental efflux function

$$E(t) = (F_\infty - F)/(F_\infty - F_o) \quad (2)$$

involving the initial signal, F_o (at $t = 0$ when the peptide is added), and the final signal, F_∞ (when all dye is released, determined upon destroying the vesicles by adding a 0.1% amount of the detergent Triton X-100) so that $E(t)$ decreases from unity towards zero upon complete depletion of the liposomes. It should be noted that this function does not necessarily decrease in proportion to the fraction of marker being still retained inside the vesicles. The latter defines a retention function $R(t)$ [22] which can be generally expressed as

$$R(t) = [(1-Q_o)/(1-Q_t)]\cdot E(t) \quad (3)$$

The static quenching factor, $Q_o = F_o/F_\infty$, is measured for vesicles without added peptide and an entrapped dye concentration c_o. In order to determine the transient quenching factor, Q_t (related to the still entrapped dye after some time of efflux) we have eventually stopped the efflux by adding an excess of empty vesicles or simply waited ($\sim$30–35 min) until the rate slowed down by itself to less than 5% fluorescence increase within 5 min. Having the external dye separated by gel filtration, the now effective average degree of quenching was measured [20,22]. This experimentally accessible value of Q_t reflects the distribution of more or less marker depleted vesicles after an elapsed efflux time t. Applying a basic pore-formation theory [33], this distribution can be quantitatively described by a single pore-retention factor ρ, i.e. the average fraction of marker retained inside a vesicle after a single pore had been activated. In the present case, where we can presume that the relaxation time of diffusional efflux through one pore, τ_o, is much smaller than our actual efflux times, we have

$$\rho = \tau_o/(\tau_p + \tau_o) \quad (4)$$

with τ_p being the average lifetime of an open pore. In the limit of $\tau_p/\tau_o \to \infty$ we arrive at the 'all-or-none' case of efflux with $\rho = 0$ where vesicles would be either full (if no pore had been activated so far) or empty (in case one or more pores had been opened). Then one has $Q_t = Q_o$ and $R(t) = E(t)$. Otherwise a graded mode of efflux would be observed with $Q_t > Q_o$ (due to partially depleted vesicles where

the quenching factor is enhanced), being equivalent to $0 < \rho < 1$ and $R(t) > E(t)$. In other words, the percentage of fluorescence increase, $1-E(t)$, would be actually larger than the percentage of released marker, $1-R(t)$.

3. Results

3.1. Peptide–lipid association

3.1.1. Neutral liposomes

Binding of MPX to POPC-vesicles and DOPC-SUV has already been investigated quantitatively in a previous report from our laboratory [27]. We have applied the same approach to the DOPC-LUV and MPP-LUV cases. Generally, a fast kinetics of the process is completed below a few seconds. Dilution of the whole system with buffer led to a change of signal reflecting a rapid repartitioning of the peptide between the aqueous and lipid moieties according to a reversible binding equilibrium. Apparently, the binding/dissociation steps take place within the subsecond range just as it was reported for the interaction of melittin [28,34] and alamethicin [35] with PC liposomes when studied by means of stopped-flow experiments.

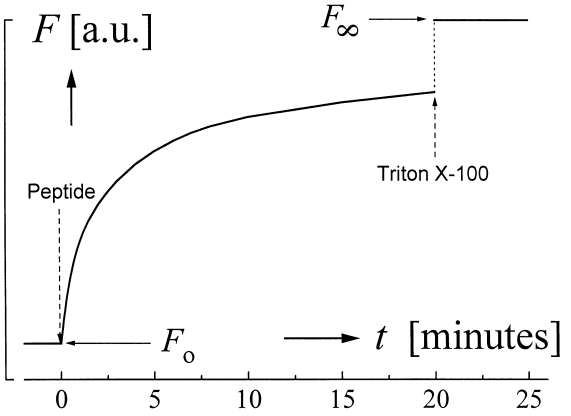

Fig. 1. A typical recording of the fluorescence signal, F (arbitrary units), versus time, t, induced by adding peptide to dye loaded vesicles at $t=0$. Due to dequenching of dye upon dilution into the external medium, F increases above the initial value, F_o, (all dye entrapped at a self-quenching concentration with a static quenching factor Q_o). After some time, the vesicles are destroyed by the detergent Triton X-100 so that the final value F_∞ (all dye being released) can be determined.

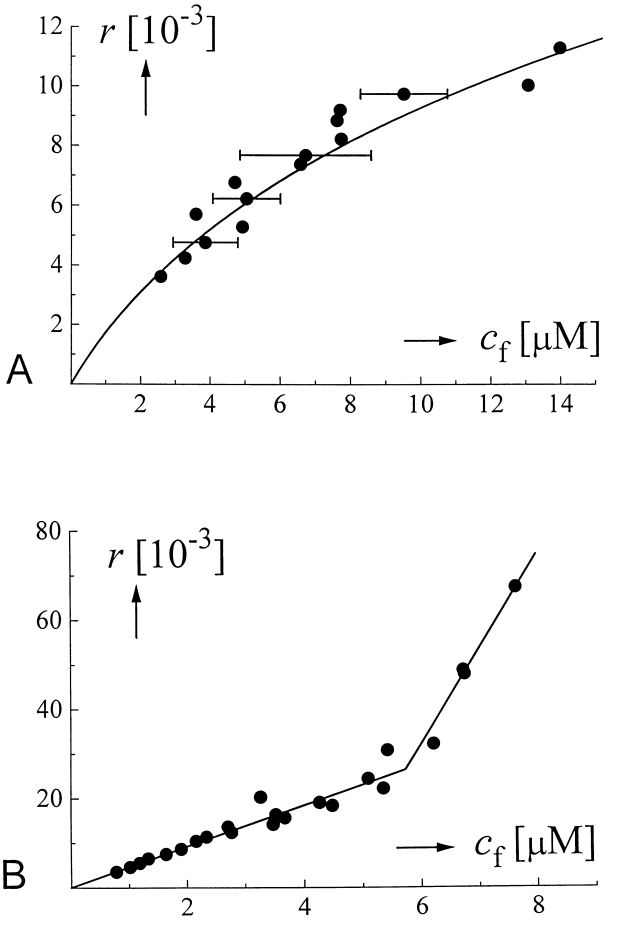

Fig. 2. Association isotherms ('binding curves') plotted as the peptide/lipid binding ratio, r, versus the free peptide concentration, c_f. The data points have been averaged over a larger number of reiterated vesicle preparations (see text). (A) Results obtained for MPX binding to DOPC-LUV. The solid curve was calculated based on Eq. 1 ($b=11.5$) with $K_p = 2.\times 10^3$ M^{-1} and $z=1.9$. (B) Results obtained for MPP and POPC−LUV. The initial linear part reflects ideal binding with $K_p = 4.6\times 10^3$ M^{-1} and $z=0$.

In Fig. 2A, the resulting association isotherm for the MPX/DOPC-LUV system is presented based on a number of experiments with a series of different vesicle preparations. We have averaged the free peptide concentrations, c_f, from up to nine measured values related to the same bound peptide/lipid ratio, r. This is indicated due to the inevitable margin of physical properties in reiterated vesicle preparations as pointed out already above. The mean data points can eventually be fitted quite well by a curve according to the functional relationship of Eq. 1 specifying a partition coefficient, K_p, and an effective charge

number, z. These parameters are compiled in Table 1 for the various systems under consideration. The partition coefficients and effective charge numbers for MPX are about the same as found for melittin [20]. These charge numbers turn out to be clearly smaller than the physical net charge of +4, a phenomenon usually observed in such cases. This has been attributed to the fact that one deals with discrete charges being not strictly localized in the exact lipid/water interface [36].

Fig. 2B features the same situation for MPP (with a physical net charge of +2) and POPC-LUV. This demonstrates a clearly different picture. Below a critical value of c_f there is a linear course of the association isotherm reflecting thermodynamically ideal association with practically no effective charge and a markedly enhanced binding affinity. The sharp upward bend beyond that range apparently points to a pronounced aggregation of bound MPP monomers similar to such an effect proposed for alamethicin [37,38] and other peptides [39,40].

3.1.2. Charged liposomes

Binding to negatively charged vesicles can be expected to be much more efficient than to the zwitterionic ones, presumably due to electrostatic attraction. We have probed this with mixed PC/PS (9:1) LUV. Interestingly, we observed there a pronounced biphasic binding kinetics. After an initial subsecond phase, a much slower additional association could be measured. The latter process extended well into the minutes range depending on the given peptide to lipid ratio. The additional association appears to be caused by a translocation of peptide molecules across the membrane. In that case, all lipid would be accessible for the peptide and the partitioning equilibrium shifted towards a larger degree of binding. This idea is supported by a translocation assay as shown by the example of Fig. 3. There is an initial jump of the signal resulting from fast binding to the outer leaflet, followed in the course of 50 min by a signal indicating that approximately half of the bound peptide has apparently reached the inner membrane side. Thus the slow part of the biphasic association kinetics could well be caused by the observed translocation process as recently suggested by Matsuzaki et al. [41]. This interesting biphasic kinetics needs a more comprehensive investigation and will not be further analyzed in the present report. With any of the neutral liposomes, only comparably negligible traces of a slow binding phase and a peptide translocation across the membrane could be seen.

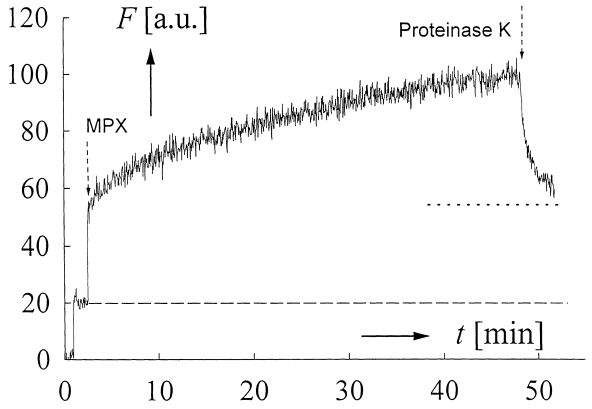

Fig. 3. Additional slow association and translocation of MPX with DOPC/POPS (9:1) and NBD-PE labeled LUV ($c_L = 51$ μM, $c_P = 6$ μM) as monitored by the fluorescence increase (arbitrary units). Arrows point to the addition of peptide and eventually 20 μM proteinase K (see text). The dashed and dotted lines indicate the signals of pure lipid (no peptide) and apparent inner leaflet peptide binding, respectively.

Table 1
Partition coefficients, K_p, and effective charge numbers, z, according to Eq. 1 determined for the mastoparan peptides upon association with the various vesicle types at pH 7.4 and 100 mM NaCl ($b = 11.5$)

Peptide	Vesicle type	K_p (10^3 M^{-1})	z
MPX	POPC-SUV[a]	24	2.4
	POPC-LUV[a]	4	2.4
	DOPC-SUV[a]	16	1.8
	DOPC-LUV	2.0	1.9
MPP	POPC-LUV	4.6	0

These parameters are subject to uncertainties of about ±30% and 15%, respectively (see text).
[a]Results adopted from [27].

3.1.3. Bilayer perturbation

A given membrane asymmetry can apparently be perturbed by pore-forming peptides [42,43]. The ability of MPX to induce an exchange of lipids between the leaflets even in zwitterionic vesicle membranes [41] was probed by us in view of a possible relation between a peptide induced structural perturbation and pore formation. We observed a rapid lipid ex-

change induced by mastoparan X using LUV asymmetrically labeled with NBD-PE (on the inner leaflet). With POPC-LUV about 30–40% of NBD-PE flipped to the outer layer in less than 1–2 min. Practically the same results were obtained for a flip-flop of NBD-PE from the outer leaflet.

3.2. Marker efflux

3.2.1. Static quenching

Carboxyfluorescein exhibits self-quenching in the mM range [18–20,22]. The static quenching factor of the dye, Q_o, when entrapped at a concentration c_o (up to about 50 mM) in our PC vesicles has been reported elsewhere [20,22]. The observed results could be very well described by an exponential function, $Q_o = \exp\{-ac_o\}$, with a characteristic parameter a. For the sake of convenience, however, we have fitted the data by a polynomial, namely

$$Q_o(c_o) = 1 + a_1 \cdot y + a_2 \cdot y^2 + a_3 \cdot y^3 \quad (5)$$

where $y = c_o/(50\ \text{mM})$ and the set of respective coefficients (a_1, a_2, a_3) is given as: (−1.84, +0.94, 0) for POPC-SUV; (−1.325, +0.487, 0) for DOPC-SUV; and (−2.95, +3.3, −1.29) for all LUV.

This choice allows a more appropriate calculation of transient quenching factors, Q_t, in terms of a single pore retention factor, ρ [22].

Spontaneous efflux that slowly leads to a decrease of Q_o was measured for the various vesicle samples under the standard efflux conditions (without a peptide). The SUV showed some irreproducible spontaneous efflux. It resulted in a linear increase of Q_o in the course of about 10 h with a $\Delta Q_o < 0.01$ per hour.

Table 2
Single pore-retention factors, ρ, for the various mastoparan–CF vesicle systems determined from measurements of the transient dequenching effect

	POPC	DOPC	DOPC/DOPS
MPX-SUV	0.1 (9)	<0.1 ($>\approx 10$)	
MPX-LUV	0.55 (0.8)	0.24 (3.2)	0.21 (3.8)
MPP-LUV	0.52 (0.9)		

Uncertainties are estimated to be about 0.05. The average pore lifetime in proportion of the relaxation time of the efflux through a single pore, τ_p/τ_o, according to Eq. 4 is given in parentheses.

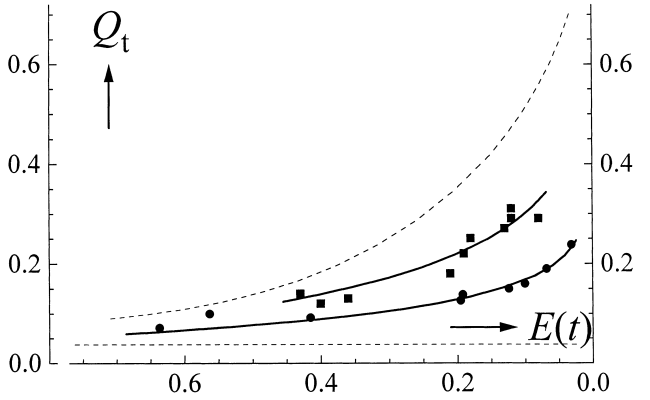

Fig. 4. Transient quenching factors, Q_t, versus the efflux function $E(t)$, in the course of dye release induced by mastoparan peptides in LUV. The curves have been calculated by means of the Eqs. 3, 5 and 6 ($Q_o = 0.04$ according to an entrapped CF concentration of 53 mM).The dashed lines indicate the two extreme cases of $\rho = 0$ ('all-or-none' mode of efflux, horizontal line) and $\rho \to 1$ (upper bound of graded efflux). The two solid curves for $\rho = 0.24$ and $\rho = 0.52$ are fits to the experimental data obtained with MPX/DOPC-LUV (●) and MPP/POPC-LUV (■), respectively.

Thus it may be neglected when the efflux experiments are carried out right after having removed external dye by gel filtration. Interestingly, we found that under the conditions of low efflux extent the increase of the CF fluorescence in the control without peptide could be higher than in the samples with peptide after approximately 1–2 h. Apparently, the bound peptide has a stabilizing effect against spontaneous efflux. Spontaneous efflux from LUV was negligible for much longer times. The static quenching factor of the extruded vesicles suspension did not change significantly during the experimental day.

3.2.2. Transient quenching

In an extension of the applied basic theory [33], the experimentally accessible value of Q_t can be related to the factor ρ, the instantaneous value of $E(t)$ and the parameters of Eq. 5 through the equation

$$Q_t = 1 + \sum_m a_m \cdot y^m \cdot [R(t)]^{z_m} \quad (m = 1, 2, 3)$$

$$\text{where } z_m = m\rho/(m + 1 - m\rho) \quad (6)$$

as described in detail previously [22]. Together with Eq. 3 the appropriate Q_t at any observed value of $E(t)$ may so be calculated for a given $\rho < 1$.

In view of this approach, we have plotted our

measured Q_t versus the respective value of $E(t)$ as shown for the two examples in Fig. 4. Evidently, the data points can quite satisfactorily be fitted by a solid curve corresponding to a specific ρ-value. The various pore retention factors as well as the average pore lifetimes in relation to τ_o are compiled in Table 2.

The order of magnitude of τ_o can be estimated assuming free diffusion of marker molecules through a water-filled cylindrical pore [44]. In the present cases (with an estimated pore diameter of some 2–3 nm, see below), this results in about 10 μs for the SUV and 2 ms for the LUV. Accordingly, the pore lifetimes in the large vesicles appear to fall in the ms range, thus being about one order of magnitude above those in the SUV.

3.2.3. Pore-formation kinetics

Leakage of marker that is induced by the mastoparans proved to be reversibly coupled to the fast peptide binding process. This is indicated by several observations. (1) The efflux was additive. Addition of either dye-loaded vesicles or peptide stock solution to a prepared peptide-vesicle suspension induced a fast efflux up to the level expected for the total peptide and lipid concentration. (2) The efflux could be stopped immediately by an excess of unloaded liposomes (at a concentration that is about five times higher than the original lipid concentration). (3) The release could also be stopped when removing bound peptide by gel filtration.

Pertinent processing of measured efflux functions was performed along the lines of the basic theory under consideration [33] that had led to the relation

$$R(t) = \exp[-(1-\rho)\cdot p(t)] \quad (7)$$

Thus we could calculate $p(t)$, the average number of pore openings per vesicle, from the empirical efflux function $E(t)$ with a pertinent value of ρ and taking into account Eq. 3. An example is presented in Fig. 5. We always observed only a few or even less than one average pore opening(s) within minutes. Generally, all such kinetic pore activation curves could very well be fitted by an integrated pore formation rate $\upsilon = dp/dt$ which comprises two single-exponential relaxation steps:

$$\upsilon = \upsilon_1\cdot\exp(-k_1 t) + \upsilon_2\cdot\exp(-k_2 t) + \upsilon_3 \quad (8)$$

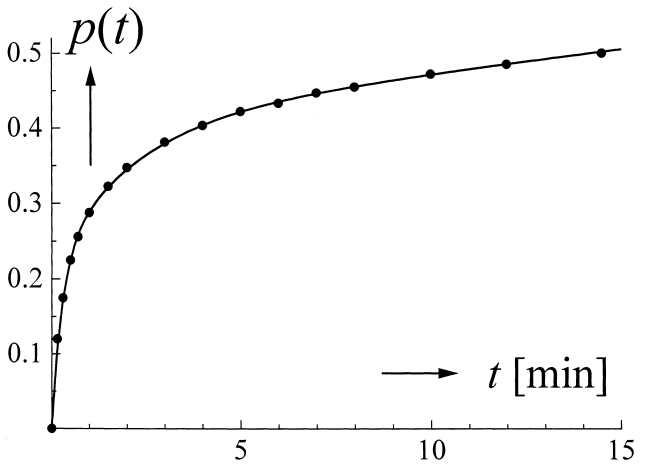

Fig. 5. Number of pore openings, $p(t)$, in the course of time calculated with Eq. 7 from an experimental efflux function with MPP acting on POPC-LUV ($c_L = 53$ μM, $c_P = 0.3$ μM; $r = 1.11\times10^{-3}$). The solid curve is a fit according to Eq. 8. The relevant time constants are $k_1 = 3.6$ min^{-1}, $k_2 = 0.45$ min^{-1}, whereas the rate amplitudes are $\upsilon_1 = 0.71$ min^{-1}, $\upsilon_2 = 0.086$ min^{-1}, $\upsilon_3 = 0.0064$ min^{-1}.

Averages of the involved five rate parameters, i.e. two time constants and three relaxation amplitudes, were investigated with regard to the bound peptide/lipid ratio, r, calculated according to Eq. 1. The peptide concentrations were in any case so small that practically ideal binding (with $\alpha = 1$) did apply. Thus the molar fraction of lipid associated peptide could be computed as

$$x_{as} = K_p c_L/(1 + K_p c_L)$$

$$\text{and subsequently } r = x_{as}\cdot(c_P/c_L) \quad (9)$$

We emphasize that our lipid concentrations were always taken so that the values of x_{as} fell between a percentage of about 20 up to less than 50. In other words, there was, in any case, an amply endowed pool of free peptide that could rapidly exchange with bound peptide.

As mentioned already, vesicle preparations are difficult to be reproduced precisely. Measurements at the same value of r have therefore been subject to a greater uncertainty of up to 30%. Within this error margin it could be quite satisfactorily established by the applied averaging procedure that the time constants k_1 and k_2 showed no significant change upon variation of r. The rate amplitudes, on the other hand, apparently increased when r was raised as

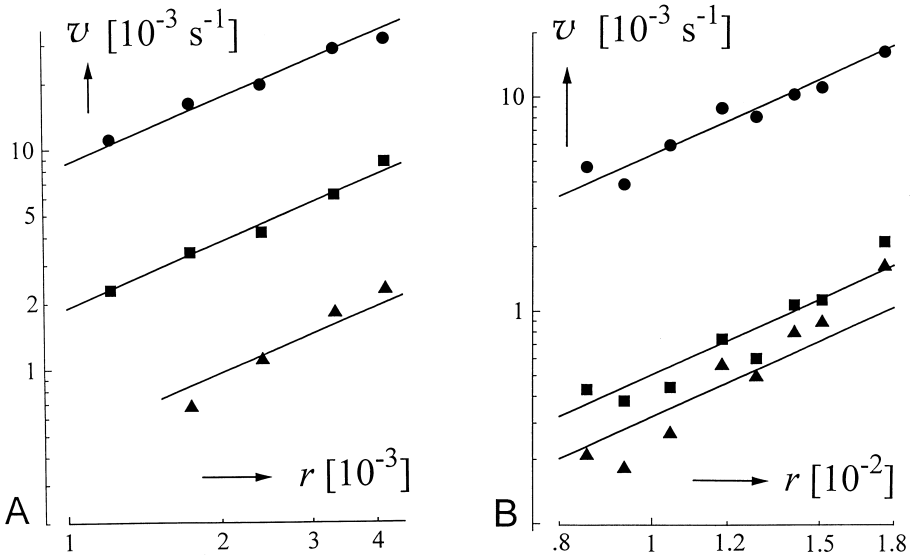

Fig. 6. Double logarithmic plots of the averaged rate amplitudes, υ_1 (●), υ_2 (■), υ_3 (▲), versus the peptide/lipid binding ratio, r. (A) MPX acting on POPC-LUV. The straight lines have a slope of 1 (indicating a first-order rate law). (B) MPX acting on POPC-SUV. The straight lines have a slope of 2 (second-order rate law).

demonstrated in Fig. 6. A rate law of the first order turned out to apply to the two MPX/LUV systems, whereas a second order was found in the other cases. The average number of bound peptide monomers per liposome was in the range of 60 to 650 for the LUV and 30 to 75 for the SUV, respectively.

When comparing pore activities on vesicles of different sizes, υ should be divided by N_L. The reduced rate $\upsilon^* = \upsilon/rN_L$ then becomes equal to the rate of pore openings per bound peptide monomer. It will be independent of r for a first-order law and proportional to r for the second-order cases. The various averages of the two time constants and three characteristic reduced rate amplitudes are compiled in Table 3. These latter quantities are υ_o^* (derived from the extrapolated initial rate $\upsilon_o = \upsilon_1 + \upsilon_2 + \upsilon_3$ at $t = 0$), the intermediate υ_i^* (from $\upsilon_2 + \upsilon_3$) and the final steady state value υ_∞^* (from the final rate υ_3).

3.2.4. Pore size

To probe the upper limit of an effluent's molecular dimensions we loaded POPC-LUV with FITC-dextran of MW 9400 at a self-quenching concentration of 23 mM. No significant peptide-induced efflux of FITC-dextran was observed. Hence we concluded, that the average diameter of a pore was smaller than 4 nm, the apparent diameter of dextran 9400 [45]. Since the CF marker molecules can be estimated to have a diameter slightly above 1 nm, a pore size in the range of 2–3 nm would be most likely, which agrees quite well with results obtained for melittin pores [46].

Table 3
Averages of the reduced pore-forming rate amplitudes (see text) for the various mastoparan–vesicle systems (experimental uncertainties are around 30%)

	k_1 (10^{-2} s^{-1})	k_2 (10^{-2} s^{-1})	υ_o^* (10^{-5} s^{-1})	υ_i^* (10^{-5} s^{-1})	υ_∞^* (10^{-5} s^{-1})
MPX/POPC-LUV	8.2	0.51	12.65	2.75	0.55
MPX/DOPC-LUV	12.9	0.66	8.57	0.52	0.13
MPX/POPC-SUV	10.8	0.46	1 690·r	160r	15.7·r
MPX/DOPC-SUV	12.7	0.50	561·r	91.4·r	31.4·r
MPP/POPC-LUV	6.5	0.68	19 300·r	2 520·r	220·r

3.2.5. Long-time resealing

We measured the extent of efflux out of the rather stable LUV after 1, 2, 6 and 8 h. When approximately 8 h had elapsed the fluorescence signal stopped to increase altogether. Below a certain critical peptide/lipid ratio it remained practically constant over 60 h at definitely less than F_∞. In other words, there was no full depletion of the vesicles' marker content, indicating total termination of further pore formation. The fraction of still entrapped dye was determined as R_∞, i.e. the value of the final retention function. For the MPX/POPC-LUV system it turned out that after a distinctly noticeable initial efflux process a complete resealing with R_∞ remaining clearly above zero was evident for an average of 20–50 bound peptide monomers (or $r \approx 2\text{–}6 \times 10^{-4}$). In that case, much less than 1% of the liposome's outer surface could have been covered with bound peptide, suggesting a pore-like action.

4. Discussion

The fact that electrically neutral lipid vesicles are able to bind the present peptides evidently indicates an affinity based on hydrophobic interactions. This can be considered to be a rather fast process. On the other hand, electrostatic interactions between the positive charges of MPX and negatively charged vesicles has been seen to result in a biphasic kinetics where an additional much slower binding reaction takes place. Our experiments suggest that this goes along with farther penetration into the bilayer, leading eventually to a translation across the membrane. Practically no such translocation does occur in our electrically neutral vesicle membranes to which we have directed the main attention in this study. By all means, however, these membranes are structurally perturbed by the peptide as indicated by a rapid lipid flip-flop.

We note that definitely a graded mode of marker efflux is indicated in most of the present cases. Accordingly, the pore lifetimes were estimated to be of the order of milliseconds or less, based on free diffusion through water-filled pores. A somewhat reduced diffusion rate due to an activation barrier at the pore would only marginally change this picture. However, an appreciable specific dye-pore interaction appears to be rather unlikely since in test experiments with a chemically quite different marker (cobalt ions) we have seen practically the same efflux curves. Anyway, pore lifetimes are one or two orders of magnitude larger in the LUV than in the SUV, suggesting a definitely larger pore stability in the less curved lipid bilayers. On the other hand, the number of pore openings remains quite small within the measuring time of minutes. Thus the average number of peptide molecules involved in an active pore will always be negligible in comparison with the bulk of bound peptide.

A rather peculiar feature of the efflux kinetics is its remarkable slowing down. This phenomenon has been generally observed with other permeabilizing agents, too. Actually, one should expect that a reversible binding process with a fast exchange of the agent between the vesicles implies a continuing pore formation everywhere. Only if there is an irreversible binding mode of the agent, the resulting Poisson statistics of distributing molecules on the individual liposomes would necessarily lead to a decreasing efflux rate as suggested by Parente et al. [47] with regard to the peptide GALA.

However, there are more general cases exhibiting fast reversible binding where nevertheless an obvious slowing down of the pore opening kinetics occurs. This clearly indicates the existence of a most favorable molecular setting for pore formation right after the moment of adding the agent that will then become more and more ineffective due to some adverse process. Such an event must be related to a transient destabilization caused by the action of the added agent as pointed out by Grant et al. [48] in the case of magainin 2a. It may be coupled with a translocation across a negatively charged membrane [49].

In our present cases involving zwitterionic vesicles, we can rule out irreversible binding as well as translocation. Actually, we deal with a situation that is largely similar to the one recently encountered with melittin [20]. After a fast binding step, the total bound peptide/lipid ratio, r, remains virtually constant over the time of measured efflux. Only a comparatively small fraction of bound peptide seems to be involved in pore-related conversions. These are reflected in two relaxation steps of the pore-opening rate. The respective time constants are seen to be practically independent of r. Thus we propose a

pore nucleation step being controlled by a passage through two rate determining intermediate states of bilayer inserted peptide monomers. Interestingly, those time constants are of about the same magnitude for melittin and the present mastoparans. Only the rate amplitudes are much smaller for the latter peptides. Anyway, however, they turn out to be of the first order also with our MPX-LUV systems. Therefore we propose basically the same scheme of reaction steps that has been advanced in the melittin case [20], namely that shown in Scheme 1.

The various A stand for monomeric states of the pore-forming agent. The k are first-order rate constants that are to apply after the initial perturbation period. The A_0 is the main binding state of monomers being always coupled with the free monomer A_{free} through a fast partitioning equilibrium. The states A_1 and A_2 are bound monomers in a structurally and/or energetically more favorable membrane penetrating position. These states are rapidly populated during the initial bilayer perturbation but will decline along Scheme 1 when the rapid bilayer perturbation has given way to a restabilization of the peptide/lipid structural arrangement. The prepore nucleus A_3 immediately undergoes a reaction towards a pore opening. Because of the established coupling to the fast binding step, this apparently involves merging with an unknown number of m additional monomers of the A_0-type. Then the rate of pore openings would be equal to the production rate of A_3. Accordingly we have

$$\upsilon = k_{23} \cdot N_L \cdot r_2 \tag{10}$$

where r_2 refers to the bound peptide/lipid ratio of A_2. Upon its fast deactivation, the pore is to equilibrate rapidly with the bulk of bound peptide (indicated as X) so that pore formation and decomposition rates cancel out each other. Furthermore, as pointed out above, we may neglect in the total amount of all bound peptide molecules those that are momentarily engaged in an active pore.

Applying standard routines of relaxation kinetics, Scheme 1 leads to two linear differential equations

$$A_{free} \overset{fast}{\rightleftharpoons} A_0 \underset{k_{10}}{\overset{k_{01}}{\rightleftharpoons}} A_1 \underset{k_{21}}{\overset{k_{12}}{\rightleftharpoons}} A_2 \overset{k_{23}}{\rightarrow} A_3 \; (+mA_0) \overset{fast}{\rightarrow} \text{pore} \rightarrow X$$

Scheme 1.

for the variables r_1 (the peptide/lipid ratio for A_1) and r_2. These can be generally solved so that the time dependence of r_2 may be inserted into Eq. 10. Eventually υ assumes the functional form of Eq. 8. The whole mathematical procedure has been described in great detail previously [20]. Here we present the final results in order to give a quantitative account of our experimental kinetics. The five rate parameters of Table 3 turn out to be related to the kinetic parameters of Scheme 1 as

$$k_1 = k_{21} + k_{23}, \quad k_2 = k_{10} + k_{12} \cdot (k_{23}/k_1) \tag{11}$$

$$\upsilon_o^* = k_{23} \cdot x_{20}, \quad \upsilon_i^* = k_{12} \cdot (k_{23}/k_1) \cdot x_{10}, \quad \upsilon_\infty^* = k_{23} \cdot x_2^\circ \tag{12}$$

This involves the initial molar fractions of bound peptide in the states A_1, A_2 ($x_{j0} = r_{j0}/r$, $j = 1,2$) and the final steady-state molar fractions $x_2^\circ = (k_{12}/k_1) \cdot x_1^\circ$, $x_1^\circ = k_{01}/k_2$. Vice versa, one can calculate the rate constants in the proposed scheme which are quantitatively consistent with the empirical data of Table 3. Generally one obtains

$$k_{23} = \upsilon_o^*/x_{20}, \quad k_{21} = k_1 - k_{23}, \quad k_{12} = \upsilon_i^* \cdot (k_1/k_{23})/x_{10} \tag{13}$$

$$k_{10} = k_2 - k_{12} \cdot (k_{23}/k_1), \quad k_{01} = \upsilon_\infty^* \cdot (k_1/k_{23}) \cdot (k_2/k_{12}) \tag{14}$$

Since we have seven unknown variables, but only five equations, there is an apparent ambiguity of a solution, allowing some arbitrary choice of x_{10} and x_{20}. Accordingly, rather low populations of the favorable A_1-, A_2-states would be sufficient to give a quantitative account of our experimental data. In the case of the MPX/POPC-LUV those initial molar fractions may be chosen as small as 0.6 and 0.2% of the total bound peptide, respectively. To present an example, let us choose 2 and 1% so that only a total of 3% would be involved in the relaxation. The various rate constants then turn out to be k_{01}, k_{10}; k_{12}, k_{21}; k_{23} (in units of 10^{-3} s^{-1}) = 0.02, 3.7; 8.9, 6.9; 12.7. In the course of time, the initial populations of A_1, A_2 level off to marginal steady-state values of only 0.4 and 0.04%, respectively.

It should also be of interest to consider for the same system how much the individual relaxation terms contribute to pore formation and marker re-

tention. This can be derived directly from the measured data. After about 10 min we have generally $p = p_1 + p_2 + \upsilon_3 \cdot t$ where $p_1 = \upsilon_1/k_1$ and $p_2 = \upsilon_2/k_2$ are the total average pore openings in the first and second relaxation steps, respectively. For $r = 10^{-3}$ (being equivalent to 87 bound peptide monomers per large liposome) one obtains $p_1 = 0.11$, $p_2 = 0.37$, and $\upsilon_3 \cdot t = 1.72$ per hour. According to Eq. 7 the fastest step leads only to a retention factor of 0.95 (i.e. 5% efflux), the intermediate step to an additional factor of 0.84, whereas the slow one results in a factor of 0.46 per every hour so that after some 6 h, depletion of vesicle marker content is practically complete. This does indeed agree with our experiments. Since the rate amplitudes are proportional to r those pore openings and efflux rates will of course substantially increase at higher degrees of peptide binding. On the other hand, our Eqs. 7 and 8, with the rate amplitude υ_3* of Table 3 do not explain the apparent resealing at low r. We note that for instance with $r = 3.5 \times 10^{-4}$ (i.e. 30 bound peptide monomers per liposome) the retention function should have dropped below 1% after around 8 h, whereas we have actually found a largely stationary R_∞ of about 70%. Thus we conclude that in the very long run even the slow step is ultimately cut out by the membrane restabilization process. Such final resealing of the membrane by bound peptide would also be in accordance with the observed decrease of spontaneous leakage.

Both the MPX/SUV as well as the MPP/LUV are of a somewhat different nature than the MPX/LUV as they exhibit a second-order law of pore formation. Anyway, the two time constants are still concentration independent, so that we can, nevertheless, use Scheme 1 to describe the kinetics. One must merely introduce a second-order rate step in the conversion of A_2 towards A_3. We therefore assume that A_2 reacts with some other bound peptide monomer forming a prepore dimer D instead of A_3. This simply requires a substitution of k_{23} by a term $k_{23}' \cdot r$ where k_{23}' is the appropriate second-order rate constant. With this replacement, everything in our treatment of Scheme 1 remains formally the same, provided one takes care to choose k_{23}' small enough to make k_1, k_2 independent of r. In the same way as pointed out above for MPX/LUV, it can so indeed be shown that the proposed kinetics with small initial populations of pertinent A_1,A_2-states does quantitatively describe the relaxation of the pore activity also in these cases.

5. Conclusions

In spite of their suspected insufficient sequence length in comparison with melittin, the mastoparans can form pore-like lesions in lipid vesicles reflecting a broad scope of similar characteristics. The apparent pores are very short-lived and their formation involves only a small fraction of the available lipid associated peptide. There is a rate-limiting prepore nucleation step fed by two coupled monomeric states which are filled up during an initial bilayer perturbation period. These monomers appear to have penetrated into the membrane to assume a structural arrangement that is more favorable to induce pores than the bulk of bound peptide. They will fade away, however, towards a final steady state in the course of a transient restabilization of the peptide/lipid bilayer structure. The time constants in that relaxation process are practically the same for melittin and the mastoparans in all the liposomes. There is only a one to two orders of magnitude lower rate of pore formation per bound mastoparan monomer (expressed as υ*). Accordingly it needs much more of these smaller peptide molecules to create an active pore, possibly due to a considerably larger number of monomers in the underlying aggregation. The finding of an apparent dimer nucleus with MPX/SUV and MPP/LUV does not very much change the picture since the observed absolute rates are nevertheless of about the same magnitude at the relevant bound peptide to lipid ratios.

Acknowledgements

This work was supported by Grant 31-042045.94 from the Swiss National Science Foundation.

References

[1] Y. Hirai, T. Xasuhura, H. Yoshida, T. Nakajima, M. Fujino, C. Kitada, A new mast cell degranulation peptide 'mastoparan' in the venom of *Vespula lewisii*, Chem. Pharm. Bull. 27 (1979) 1942–1944.

[2] Y. Hirai, M. Kuwada, T. Yasuhura, H. Yoshida, T. Nakajima, A new mast cell degranulating peptide homologous to mastoparan in the venom of Japanese hornet (*Vespa xanthoptera*), Chem. Pharm. Bull. 27 (1979) 1945–1946.
[3] Y. Hirai, Y. Ueno, T. Yasuhura, H. Yoshida, T. Nakajima, A new mast cell degranulating peptide, polistes mastoparan, in the venom of *Polistes jadwigae*, Biomed. Res. 1 (1980) 185–187.
[4] T. Higashijima, S. Uzu, T. Nakajima, E.M. Ross, Mastoparan, a peptide toxin from wasp venom, mimics receptors by activating GTP-binding regulatory proteins (G-proteins), J. Biol. Chem. 263 (1988) 6491–6494.
[5] A. Argiolas, J.J. Pisano, Facilitation of phospholipase A2 activity by mastoparans, a new class of mast cell degranulating peptides from wasp venom, J. Biol. Chem. 258 (1983) 13697–13702.
[6] P.J. Weidmann, W.M. Winter, The G-protein-activating peptide, mastoparan and the synthetic NH_2-terminal ARF peptide, ARFp13, inhibit in vitro Golgi transport by irreversibly damaging membranes, J. Biol. Chem. 127 (1994) 1815–1827.
[7] T. Katsu, M. Kuroko, T. Morikawa, K. Sanchike, H. Yamanaka, S. Shinoda, Y. Fujita, Interaction of wasp venom mastoparan with biomembranes, Biochim. Biophys. Acta 1027 (1990) 185–190.
[8] D.R. Pfeiffer, T.I. Gudz, S.A. Novgorodov, W.L. Erdahl, The peptide mastoparan is a potent facilitator of the mitochondrial permeability transition, J. Biol. Chem. 270 (1995) 4923–4932.
[9] A. Arbuzova, G. Schwarz, Pore kinetics of mastoparan peptides in large unilamellar lipid vesicles, Progr. Colloid Polym. Sci. 100 (1996) 345–360.
[10] C.E. Dempsey, The action of melittin on membranes, Biochim. Biophys. Acta 1031 (1990) 143–161.
[11] T. Higashijima, K. Wakamatsu, J. Takemitsu, M. Fujino, T. Nakajima, T. Miyazawa, Conformational change of mastoparan from wasp venom on binding with phosopholipid membrane, FEBS Lett. 152 (1983) 227–230.
[12] K. Wakamatsu, A. Okada, T. Miyazawa, M. Ohya, T. Higashijima, Membrane-bound conformation of mastoparan-X, a G-protein-activating peptide, Biochemistry 31 (1992) 5654–5660.
[13] M.S.-P. Sansom, The biophysics of peptide models of ion channels, Progr. Biophys. Mol. Biol. 55 (1991) 139–235.
[14] D.M. Ojcius, J.D.-E. Young, Cytolytic pore-forming proteins and peptides: is there a common structural motif?, Trends Biochem. Sci. 16 (1991) 225–229.
[15] D. Marsh, Peptide models for membrane channels, Biochem. J. 315 (1996) 345–361.
[16] I.R. Mellor, M.S.P. Sansom, Ion-channel properties of mastoparan, a 14-residue peptide from wasp venom, and of MP3, a 12-residue analogue, Proc. R. Soc. Lond. B 239 (1990) 383–400.
[17] D. Eisenberg, R.M. Weiss, T.C. Terwilliger, The helical hydrophobic moment: a measure of the amphilicity of a helix, Nature 299 (1982) 371–374.
[18] J.N. Weinstein, S. Yoshikami, P. Henkart, R. Blumenthal, W.A. Hagins, Liposome-cell interaction: transfer and intercellular release of a trapped fluorescent marker, Science 195 (1977) 489–492.
[19] J.N. Weinstein, R.D. Klausner, T. Innerarity, E. Ralston, R. Blumenthal, Phase transition release, a new approach to the interaction of proteins with lipid vesicles. Application to lipoproteins, Biochim. Biophys. Acta 647 (1981) 270–284.
[20] S. Rex, G. Schwarz, Quantitative studies on the melittin-induced leakage mechanism of lipid vesicles, Biochemistry 37 (1998) 2336–2345.
[21] C.J.F. Böttcher, C.M. Van Gent, C. Fries, A rapid and sensitive sub-micro phosphorous determination, Anal. Chim. Acta 24 (1961) 203–204.
[22] G. Schwarz, A. Arbuzova, Pore kinetics reflected in the dequenching of a lipid vesicle entrapped fluorescent dye, Biochim. Biophys. Acta 1239 (1995) 51–57.
[23] M.J. Hope, M.B. Bally, G. Webb, P.R. Cullis, Production of large unilamellar vesicles by a rapid extrusion procedure. Characterisation of size distribution, trapped volume and ability to maintain a membrane potential, Biochim. Biophys. Acta 812 (1985) 55–65.
[24] L.D. Mayer, M.J. Hope, P.R. Cullis, Vesicles of variable sizes produced by a rapid extrusion procedure, Biochim. Biophys. Acta 858 (1986) 161–168.
[25] C. Huang, J.T. Mason, Geometric packing constraints in egg phosphatidylcholine vesicles, Proc. Natl. Acad. Sci. USA 75 (1978) 308–310.
[26] J.C. McIntyre, R.G. Sleight, Fluorescence assay for phospholipid membrane asymmetry, Biochemistry 30 (1991) 11819–11827.
[27] N. Hellmann, G. Schwarz, Peptide-liposome association. A critical investigation with mastoparan X, Biochim. Biophys. Acta 1369 (1998) 267–277.
[28] G. Schwarz, G. Beschiaschvili, Thermodynamic and kinetic studies on the association of melittin with a phospholipid bilayer, Biochim. Biophys. Acta 979 (1989) 82–90.
[29] G. Schwarz, U. Blochmann, Association of the wasp venom peptide mastoparan with electrically neutral lipid vesicles, FEBS Lett. 318 (1993) 172–176.
[30] G. Schwarz, Electrical interaction of membrane active peptides at lipid/water interfaces, Biophys. Chem. 58 (1996) 67–73.
[31] M. Maduke, D. Roise, Import of a mitochondrial presequence into protein-free phospholipid vesicles, Science 260 (1993) 364–367.
[32] K. Matsuzaki, O. Murase, N. Fujii, K. Miyajima, An antimicrobial peptide, magainin 2, induced rapid flip-flop of phospholipids coupled with pore formation and peptide translocation, Biochemistry 35 (1996) 11361–11368.
[33] G. Schwarz, C.H. Robert, Kinetics of pore-mediated release of marker molecules from liposomes or cells, Biophys. Chem. 42 (1992) 291–296.
[34] K.M. Sekharam, T.D. Bradrick, S. Georghiu, Kinetics of melittin binding to phospholipid small unilamellar vesicles, Biochim. Biophys. Acta 1063 (1991) 171–174.

[35] G. Schwarz, H. Gerke, V. Rizzo, S. Stankowski, Incorporation kinetics in a membrane, studied with the pore-forming peptide alamethicin, Biophys. J. 52 (1987) 685–692.
[36] S. Stankowski, Surface charging by large multivalent molecules. Extending the standard Gouy–Chapman treatment, Biophys. J. 60 (1991) 341–351.
[37] G. Schwarz, S. Stankowski, V. Rizzo, Thermodynamic analysis of incorporation and aggregation in a membrane: application to the pore forming peptide alamethicin, Biochim. Biophys. Acta 861 (1986) 141–151.
[38] V. Rizzo, S. Stankowski, G. Schwarz, Alamethicin incorporation in lipid bilayers: a thermodynamic study, Biochemistry 26 (1987) 2751–2759.
[39] D. Rapaport, Y. Shai, Interaction of fluorescently labeled pardaxin and its analogues with lipid bilayers, J. Biol. Chem. 266 (1991) 23769–23775.
[40] E. Gazit, Y. Shai, Structural and functional characterizationof the α5 segment of bacillus thuringiensis δ-endotoxin, Biochemistry 32 (1993) 3429–3436.
[41] K. Matsuzaki, S. Yoneyama, O. Murase, K. Miyajima, Transbilayer transport of ions and lipids coupled with mastoparan X translocation, Biochemistry 35 (1996) 8450–8456.
[42] P.F. Devaux, Static and dynamic asymmetry in cell membranes, Biochemistry 30 (1991) 1163–1173.
[43] E. Fattal, S. Nir, R.A. Parente, F.C. Szoka Jr., Pore-forming peptides induce rapid phospholipid flip-flop lin membranes, Biochemistry 33 (1994) 6721–6731.
[44] G. Schwarz, C.H. Robert, Pore formation kinetics in membranes, determined from the release of marker molecules out of liposomes or cells, Biophys. J. 58 (1990) 577–583.
[45] M.P. Bohrer, W.M. Deen, C.R. Robertson, J.L. Troy, B.M. Brenner, Influence of molecular configuration on the passage of macromolecules across the glomerular wall, J. Gen. Physiol. 74 (1979) 583–593.
[46] A.S. Ladokhin, M.E. Selsted, S.H. White, Sizing membrane pores in lipid vesicles by leakage of co-encapsulated markers: pore formation by melittin, Biophys. J. 72 (1997) 1762–1766.
[47] R.A. Parente, S. Nir, F.C. Szoka Jr., Mechanism of leakage of phospholipid vesicle contents induced by the peptide GALA, Biochemistry 29 (1990) 8720–8728.
[48] E. Grant Jr., T.J. Beeler, K.M.P. Taylor, K. Gable, M.A. Roseman, Mechanism of magainin 2a induced permeabilization of phospholipid vesicles, Biochemistry 31 (1992) 9912–9918.
[49] K. Matsuzaki, O. Murase, N. Fujii, K. Miyajima, Translocation of a channel-forming antimicrobial peptide, magainin 2, across lipid bilayers by forming a pore, Biochemistry 34 (1995) 6521–6526.